

# Primary charge separation in the bacterial reaction center: Validity of incoherent sequential model

Michal Pudlak<sup>a)</sup>

*Institute of Experimental Physics, Slovak Academy of Sciences, Watsonova 47, 043 53 Košice, Slovak Republic*

(Received 11 April 2002; accepted 30 October 2002)

A description of electron transfer (ET) by the incoherent sequential model was employed to elucidate the unidirectionality of the primary charge separation process in bacterial reaction centers (RC). The model assumes that the vibrational relaxation of the medium modes is sufficiently fast and that the system relaxes to thermal equilibrium after each ET step. ET was investigated for 5-sites (molecules) arranged in two branches. Beginning at molecule 1, ET can proceed in two directions with each branch composed of two molecules. Analysis shows that the model can successfully explain the asymmetry of primary electron transfer both in the wild type and several mutants of Rb capsulatus RC. In these cases the dependence of ET asymmetry on temperature was also evaluated. It was shown that in order to obtain the correct temperature dependence of ET asymmetry in the mutants, the superexchange mechanism operating in parallel with the sequential process must be used. © 2003 American Institute of Physics. [DOI: 10.1063/1.1531630]

## I. INTRODUCTION

The problem of bacterial photosynthesis has attracted much interest since the reaction center (RC) of bacteria provides an interesting system for studying a high-efficiency electron transfer in an organized molecular complex. The photosynthetic reaction center<sup>1</sup> is a special pigment-protein complex, which functions as a photochemical trap. The reaction centers (RC) of a purple bacteria are composed of three protein subunits called *L*, *M*, and *H*.<sup>2,3</sup> All cofactors involved in the ET are noncovalently bound to subunits *L* and *M* in two chains. Both chains of cofactors start at the bacteriochlorophyll dimer (*P*) which is interacting with both subunits *L* and *M*. Then the cofactor chains are split and each individual one continues on subunit *L* and symmetrically on subunit *M*. Cofactors in subunit *L* are accessory bacteriochlorophyll (*B<sub>L</sub>*), bacteriopheophytin (*H<sub>L</sub>*), and quinone (*Q<sub>L</sub>*). Identically in the *M* subunit are the accessory bacteriochlorophyll (*B<sub>M</sub>*), bacteriopheophytin (*H<sub>M</sub>*), and quinone (*Q<sub>M</sub>*). The arrangement of cofactors shows the local twofold symmetry. For more details on structural arrangement, see Ref. 4.

The cofactors serve as donor-acceptor pairs in the electron transfer. In spite of the structural symmetry, the RC is functionally highly asymmetric. To describe the asymmetry of ET it was assumed that the first step of primary ET in bacterial photosynthesis has hot character.<sup>5,6</sup> This means that ET transfer is so fast that system does not have sufficient time to relax to the thermal equilibrium (stochastic fluctuations do not depend on the localization of the electrons in the branch). In this paper we attempt to analyze the possibility that ET asymmetry can be described by an incoherent sequential model which assumes, contrary to the previous model, that there exists the vibrational modes which has a sufficient time for relax to the equilibrium.

## II. MODEL

We start by considering an electron transfer system in which the electron has *N* accessible sites, embedded in a medium. We denote by  $|j\rangle$  the state with electron localized at the *j*th site and  $j=1,2,\dots,N$ . The *j* and *k* sites are coupled by  $V_{jk}$ . The interaction of the solvent with the system depends on the electronic state  $|j\rangle$  and we denote the medium Hamiltonian in the state  $|j\rangle$  by  $H_j$ . The total model Hamiltonian for the system and medium is

$$H = H_0 + V, \quad (1)$$

where

$$H_0 = \sum_{j=1}^N |j\rangle [\epsilon_j - i\Gamma_j + H_j] \langle j|, \quad (2)$$

$$V = \sum_{\substack{j,k=1 \\ j \neq k}}^N V_{jk} |j\rangle \langle k|, \quad (3)$$

where  $\epsilon_j$  is the site energy. The parameter  $\hbar/2\Gamma_j$  has a meaning of the lifetime of the electron at site *j* in the limit of the zero coupling parameter. It can characterize the possibility of the electron escape from the system by another channel for instance a nonradiative internal conversion or recombination process.

The Hamiltonian describing the reservoir consist of harmonic oscillators is

$$H_j = \sum_{\alpha} \left\{ \frac{p_{\alpha}^2}{2m_{\alpha}} + \frac{1}{2} m_{\alpha} \omega_{\alpha}^2 (x_{\alpha} - d_{j\alpha})^2 \right\}. \quad (4)$$

Here,  $m_{\alpha}$  and  $\omega_{\alpha}$  are the frequency and the mass of the  $\alpha$ th oscillator, and  $d_{j\alpha}$  is the equilibrium configuration of the  $\alpha$ th oscillator when the system is in the electronic state  $|j\rangle$ . The total density matrix  $\rho(t)$  of the ET system and the medium satisfies the Liouville equation,

<sup>a)</sup>Fax: +421 95 6336292; Electronic mail: pudlak@saske.sk

$$\partial_t \rho(t) = -\frac{i}{\hbar} [H\rho(t) - \rho(t)H^+] \equiv -iL\rho(t). \quad (5)$$

In the interacting picture,

$$\rho_I(t) = \exp\left(\frac{i}{\hbar}H_0t\right)\rho(t)\exp\left(-\frac{i}{\hbar}H_0^+t\right). \quad (6)$$

The Liouville equation in the interacting picture has the following form:

$$\begin{aligned} \partial_t \rho_I(t) &= -\frac{i}{\hbar} [V_I(t)\rho_I(t) - \rho_I(t)V_I^+(t)] \\ &\equiv -iL(t)\rho_I(t), \end{aligned} \quad (7)$$

where

$$V_I(t) = \exp\left(\frac{i}{\hbar}H_0t\right)V\exp\left(-\frac{i}{\hbar}H_0^+t\right). \quad (8)$$

Here we denote the total trace, and the partial traces over the ET system and over the medium by  $\text{Tr}$ ,  $\text{Tr}^e$ ,  $\text{Tr}^Q$ , respectively. By definition  $\text{Tr} \equiv \text{Tr}^Q \text{Tr}^e$ . The population on state  $|j\rangle$  at time  $t$  is given by

$$P_j(t) = \text{Tr}(|j\rangle\langle j|\rho(t)). \quad (9)$$

We assume that vibrational relaxation is sufficiently rapid so that the system can relax to thermal equilibrium after each ET step. This assumption determines a choice of projector operator. The projector operator  $D$  acting on an arbitrary operator  $B$  in the Hilbert space of the total ET system and medium is defined by<sup>7</sup>

$$DB = \sum_{j=1}^N \text{Tr}(|j\rangle\langle j|B)\rho_j|j\rangle\langle j|, \quad (10)$$

where  $\rho_j$  is the equilibrium medium density matrix in the state  $|j\rangle$ , i.e.,

$$\rho_j = \exp(-H_j/k_B T) / \text{Tr}^Q\{\exp(-H_j/k_B T)\}. \quad (11)$$

One can show, using Eqs. (9)–(10) that

$$DL(t)D = 0. \quad (12)$$

Using the standard projection operator techniques<sup>8,9</sup> we can derive a generalized master equation for the populations,

$$\begin{aligned} \partial_t P_j(t) &= -\frac{2\Gamma_j}{\hbar} P_j(t) - \sum_{\substack{k=1 \\ (k \neq j)}}^N \int_0^t W_{jk}(t-\tau) P_j(\tau) d\tau \\ &+ \sum_{\substack{k=1 \\ (k \neq j)}}^N \int_0^t W_{kj}(t-\tau) P_k(\tau) d\tau \quad j=1, \dots, N, \end{aligned} \quad (13)$$

where

$$\begin{aligned} W_{jk}(t) &= 2 \frac{|V_{jk}|^2}{\hbar^2} \text{Re} \left\{ \exp\left[-\frac{\Gamma_j + \Gamma_k}{\hbar} t\right] \exp\left[\frac{i(\epsilon_j - \epsilon_k)}{\hbar} t\right] \right. \\ &\times \exp\left\{ \sum_{\alpha} \frac{E_{jk}^{\alpha}}{\hbar \omega_{\alpha}} [(\bar{n}_{\alpha} + 1)e^{-i\omega_{\alpha}t} \right. \\ &\left. \left. + \bar{n}_{\alpha} e^{i\omega_{\alpha}t} - (2\bar{n}_{\alpha} + 1)] \right\} \right\}. \end{aligned} \quad (14)$$

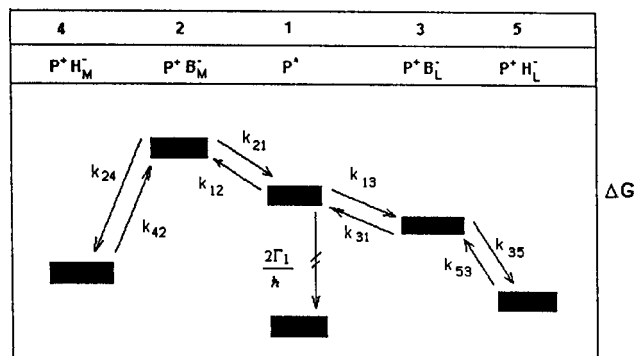


FIG. 1. Kinetic scheme for the primary electron transfer in bacterial photosynthetic reaction centers.

Here,  $\bar{n}_{\alpha} = [\exp(\hbar \omega_{\alpha}/k_B T) - 1]^{-1}$  is a thermal population of the  $\alpha$ th mode and

$$E_{jk}^{\alpha} = \frac{1}{2} m_{\alpha} \omega_{\alpha}^2 (d_{j\alpha} - d_{k\alpha})^2 \quad (15)$$

is the reorganization energy of the  $\alpha$ th mode when system transfers from state  $|j\rangle$  to state  $|k\rangle$ .

### III. MODEL OF RC

To describe the first steps of electron transfer processes in the reactions centers we have used the 5-sites model. We designate the special pair ( $P$ ) as site 1, the sites 2 and 3 represent the molecules  $B_M$  and  $B_L$ , the sites 4 and 5 then represent the molecules  $H_M$  and  $H_L$  (Fig. 1). We consider that this system is coupled to a bath (medium).

Based on experimental observations of ET in RC it is expected that bacteriochlorophyll play a crucial role in ET. In this model we assume that ET in RC is sequential where the  $P^+ B^-$  state on both sides is a real chemical intermediate. In addition, the repopulation of accessory bacteriochlorophylls from molecules of bacteriopheophytin is negligible because of the large energy difference between these states. The imaginary part of energy level 1 describes the probability of electron deactivation to the ground state. With these assumptions Eq. (13) has the form,

$$\begin{aligned} \partial_t P_1(t) &= -\frac{2\Gamma_1}{\hbar} P_1(t) - \int_0^t W_{12}(t-\tau) P_1(\tau) d\tau \\ &+ \int_0^t W_{21}(t-\tau) P_2(\tau) d\tau \\ &+ \int_0^t W_{31}(t-\tau) P_3(\tau) d\tau \\ &- \int_0^t W_{13}(t-\tau) P_1(\tau) d\tau, \end{aligned} \quad (16a)$$

$$\begin{aligned} \partial_t P_2(t) &= -\int_0^t W_{21}(t-\tau) P_2(\tau) d\tau + \int_0^t W_{12}(t-\tau) \\ &\times P_1(\tau) d\tau - \int_0^t W_{24}(t-\tau) P_2(\tau) d\tau, \end{aligned} \quad (16b)$$

$$\begin{aligned} \partial_t P_3(t) = & - \int_0^t W_{31}(t-\tau) P_3(\tau) d\tau + \int_0^t W_{13}(t-\tau) \\ & \times P_1(\tau) d\tau - \int_0^t W_{35}(t-\tau) P_3(\tau) d\tau. \end{aligned} \quad (16c)$$

To neglect the repopulations of electron accepting sites requires an introduction of imaginary parts of energy levels for these sites. Without the imaginary part we would have incorrect equations resulting, for instance, in negative occupation probabilities.<sup>10</sup>

#### IV. ELECTRONIC ESCAPE THROUGH THE BRANCHES

The quantum yields  $\Phi_L$ ,  $\Phi_M$  of electronic escape via branch  $L$ ,  $M$  and the quantum yields  $\Phi_G$  of direct ground state recombination can be characterized by the expressions

$$\Phi_G = \frac{2\Gamma_1}{\hbar} \int_0^\infty P_1(t) dt = \frac{2\Gamma_1}{\hbar} P_1(s \rightarrow 0^+), \quad (17a)$$

$$\begin{aligned} \Phi_M = & \int_0^\infty \int_0^t W_{24}(t-\tau) P_2(\tau) d\tau dt \\ = & k_{24}(s \rightarrow 0^+) P_2(s \rightarrow 0^+), \end{aligned} \quad (17b)$$

$$\begin{aligned} \Phi_L = & \int_0^\infty \int_0^t W_{35}(t-\tau) P_3(\tau) d\tau dt \\ = & k_{35}(s \rightarrow 0^+) P_3(s \rightarrow 0^+), \end{aligned} \quad (17c)$$

where  $P_i(s)$ ,  $k_{ij}(s)$  are the Laplace transformation of  $P_i(t)$  and  $W_{ij}(t)$ . The quantum yields (QY) must fulfill the relation

$$\Phi_G + \Phi_L + \Phi_M = 1. \quad (18)$$

Parameters  $K$  and  $R$  defined by equations

$$K = \frac{\Phi_L}{\Phi_M}, \quad (19a)$$

$$R = \frac{\Phi_L}{\Phi_G}, \quad (19b)$$

express the asymmetry in probabilities of electronic escape through branches  $L$  and  $M$ .  $K$  is a ratio of electron escape through the  $L$  and  $M$  side and  $R$  is the ratio of electron escape via  $L$  side to the ground state recombination. For our goals these two parameters are of principal importance.

Assuming that at initial conditions,

$$P_1(0) = 1, \quad P_2(0) = P_3(0) = 0,$$

we can solve Eq. (16) by Laplace transformation. The solution gives us

$$K = \frac{k_{13} \left[ \exp\left(-\frac{G_{12}}{k_B T}\right) k_{12} + k_{24} \right] k_{35}}{k_{12} \left[ \exp\left(-\frac{G_{13}}{k_B T}\right) k_{13} + k_{35} \right] k_{24}}, \quad (20a)$$

$$R = \frac{k_{13} k_{35}}{2\Gamma_1 \left[ \exp\left(-\frac{G_{13}}{k_B T}\right) k_{13} + k_{35} \right]}. \quad (20b)$$

Here we denote  $k_{ij}(s \rightarrow 0^+)$  as  $k_{ij}$ .

Now we analyze some special cases of ET in the RC. In case when backward ET from sites 2 and 3 are much greater than  $k_{24}$  and  $k_{35}$  we get

$$K = \exp\left(\frac{G_{23}}{k_B T}\right) \frac{k_{35}}{k_{24}}, \quad R = \frac{\hbar k_{35}}{2\Gamma_1} \exp\left(\frac{G_{13}}{k_B T}\right). \quad (21)$$

It means that with small constants  $k_{24}$  and  $k_{35}$  the system can reach a quasiequilibrium and a unidirectionality is modified mainly by the Boltzmann factors. It does not depend on the electronic couplings  $V_{12}$  and  $V_{13}$ .

In the opposite case, when backward reactions are slow in comparison to constants  $k_{24}$  and  $k_{35}$  we have  $K = k_{13}/k_{12}$  and  $R = \hbar k_{13}/2\Gamma_1$ . The form of parameter  $K$  is the same as one used to characterize the unidirectionality in an earlier study.<sup>11</sup>

We assume that the memory functions, which characterize ET, can be described by both a low frequency medium vibrational mode and a high frequency intramolecular vibrational mode. At a high temperature regime the constant  $k_{ij}(s \rightarrow 0^+)$  is in the form<sup>12</sup>

$$\begin{aligned} k_{ij} = & \int_0^\infty W_{ij}(t) dt \\ = & \frac{2\pi}{\hbar} V_{ij}^2 \left( \frac{1}{4\pi\lambda_{ij}k_B T} \right)^{1/2} \exp(-S_{ij}) \\ & \times \sum_{n=0}^\infty \frac{S_{ij}^n}{n!} \exp\left[ \frac{(G_{ji} + \lambda_{ij} + n\hbar\omega_{ij})^2}{4\lambda_{ij}k_B T} \right]. \end{aligned} \quad (22)$$

Here,  $G_{ij} = \epsilon_i - \epsilon_j$  and

$$S_{ij} = \frac{1}{2} m_{cij} \omega_{ij} (d_{ci} - d_{cj})^2 / \hbar \quad (23)$$

is the scaled reorganization constant for the high frequency  $ij$ th mode when the electron is transferred from state  $|i\rangle$  to state  $|j\rangle$ , and

$$\lambda_{ij} = \frac{1}{2} m_{mij} \omega_{mij}^2 (d_{mi} - d_{mj})^2 \quad (24)$$

is the reorganization energy of the low-frequency mode when electron transferred from state  $|i\rangle$  to state  $|j\rangle$ . In derivation of constants  $k_{12}$ ,  $k_{13}$  it was assumed that  $\Gamma_1 \ll \hbar\omega_{12}$ ,  $\hbar\omega_{13}$ .

To solve Eq. (13) the inverse Laplace transformation of  $P_i(s)$  has to be applied and for this purpose a complete frequency dependence of  $k_{ij}(s)$  is needed. Changing Eq. (13) to the ordinary rate equation, where the constants  $k_{ij}$  are employing as a rate constants, gives the solutions for the population probabilities  $P_i(t)$  which are different from the exact solution of Eq. (13). The solution of  $P_i(t)$  from the ordinary rate equations which employ constant  $k_{ij}$  as a rate constant may even yield a negative population in the short time scales.<sup>13</sup> In the longer time scales it is assumed that these equations approach the exact solutions. However, it was shown that it is not generally true.<sup>14</sup>

TABLE I. Computed constants  $1/k_{ij}$  and quantum yields for wild type and mutant RC's.<sup>a</sup>

Sample	$T$ (K)	$\epsilon_2$ ( $\text{cm}^{-1}$ )	$\epsilon_3$ ( $\text{cm}^{-1}$ )	$\epsilon_4$ ( $\text{cm}^{-1}$ )	$\epsilon_5$ ( $\text{cm}^{-1}$ )	$1/k_{12}$ (ps)	$1/k_{24}$ (ps)	$1/k_{13}$ (ps)	$1/k_{35}$ (ps)	$\phi_L$	$\phi_M$	$\phi_G$
WT	295	800	-450	-1000	-2000	96.7	1.02	2.35	0.9	0.97	0.016	0.014
WT	200					508	1.2	2.1	1.1	0.985	0.002	0.013
D	295	800	480	-1000	-2000	96.7	1.02	23.7	1.15	0.688	0.167	0.145
D	200					508	1.2	64	1.01	0.598	0.064	0.338
DH	295	800	480	-1000	-1000	96.7	1.02	23.7	0.85	0.7	0.16	0.14
DH	200					508	1.2	64	1.02	0.6	0.06	0.34
KDH	295	700	480	-1000	-1000	60.3	1	23.7	0.85	0.64	0.23	0.13
KDH	200					253	1.2	64	1.02	0.56	0.12	0.32
YFH	295	550	400	-1000	-1000	31.4	0.9	17.5	0.8	0.6	0.31	0.09
YFH	200					96.8	1.1	41	0.9	0.57	0.21	0.22

<sup>a</sup>The site energy  $\epsilon_1 = 0$ . Sequential mechanism on both branches was assumed.

## V. RESULTS

The implementation of the theory requires an information regarding the energetic parameters, the medium reorganization energies, the high frequency modes, and electronic coupling terms. Several sets of parameters were used to describe a charge transfer in the RC. A set of parameters based on molecular dynamics simulations<sup>15</sup> corresponds to a dominance of superexchange mechanisms for the primary ET reaction in RCs. Another set of parameters<sup>16,17</sup> was used to fit experimental data. This second set of parameters derives a dominant contribution from the sequential mechanism. The first set of parameters has the larger reorganization energies and the greater coupling factors. This set of parameters makes the ET rate much larger than is found in the wild-type proteins.

### A. Sequential model

First, we assume that ET has sequential character in both branches of RC. Because ET kinetics in *Rb.capsulatus* is similar to kinetics of *Rb.sphaeroides*, we adapt in this work the set of parameters that characterizes the observed *L*-side experimental kinetics of *Rb.sphaeroides* RC very well.<sup>16,17</sup> The following parameters were used to describe the electron transfer in the *L* branch of the wild type of reaction centers: the values  $\hbar\omega_{13} = \hbar\omega_{35} = 1500 \text{ cm}^{-1}$  for the high frequency modes, values  $V_{13} = 32 \text{ cm}^{-1}$ ,  $V_{35} = 59 \text{ cm}^{-1}$  for the electronic couplings,  $S_{13} = S_{35} = 0.5$  for the scaled reorganization constants, and  $\lambda_{13} = \lambda_{35} = 800 \text{ cm}^{-1}$ . The following values of the free energies of the redox states 1,3,5 were chosen:  $\epsilon_1 = 0$ ,  $\epsilon_3 = -450 \text{ cm}^{-1}$ ,  $\epsilon_5 = -2000 \text{ cm}^{-1}$ . The  $P^*$  internal conversion rate is  $2\Gamma_1/\hbar = (170 \text{ ps})^{-1}$ .

Much less is known about parameters characterizing the *M*-side of the RC. It is thought that both  $P^+H_M^-$  and  $P^+B_M^-$  are at higher free energy than their *L*-side counterparts.<sup>18-22</sup> Calculations place  $P^+H_M^-$  at least  $1000 \text{ cm}^{-1}$  above  $P^+H_L^-$  (Refs. 18 and 19) and  $P^+B_M^-$  above  $P^+B_L^-$  by  $1200-2800 \text{ cm}^{-1}$ .<sup>18-22</sup> We assume that the main asymmetry between the *L* and *M* side of the RC is in the energy levels of accessory bacteriochlorophylls. For a present study the following parameters were selected to describe the electron transfer in the *M* branch of the wild type of reaction centers: the values  $\hbar\omega_{12} = \hbar\omega_{24} = 1500 \text{ cm}^{-1}$  for the high frequency modes, values  $V_{12} = 32 \text{ cm}^{-1}$ ,  $V_{24} = 59 \text{ cm}^{-1}$  for the electronic cou-

plings,  $S_{12} = S_{24} = 0.5$  for the scaled reorganization constants and  $\lambda_{12} = \lambda_{24} = 800 \text{ cm}^{-1}$ . Values of the free energies of the redox states 2 and 4 were chosen:  $\epsilon_2 = 800$ ,  $\epsilon_4 = -1000 \text{ cm}^{-1}$ . The results of our numerical computations for wild type (WT) and mutant RC's are collected in Table I. In both branches only the sequential mechanism was assumed.

Based on *Rb.capsulatus* RC mutants<sup>23,24</sup> it was suggested that the L(M212)H mutation (denoted  $\beta$ ) raises a free energy of  $P^+H_L^-$  roughly to the free energy level of  $P^+H_M^-$ . We expect that the value  $\epsilon_5 = -1000 \text{ cm}^{-1}$  should correctly characterize these mutants. G(M201)D/L(M212)H of *Rb.capsulatus* RC double mutant (denoted DH) shows 15% of ET to *M*-side bacteriopheophytin, 70% to the *L*-side cofactors, and 15% was deactivated to the ground state. The suggested model for the DH mutant assumed that the G(M201)D mutation increases a free energy of  $P^+B_L^-$  above  $P^*$  (Ref. 25) and so we had to increase the energy  $\epsilon_3$  from the value  $\epsilon_3 = -450 \text{ cm}^{-1}$  to the value  $\epsilon_3 = 480 \text{ cm}^{-1}$ . With this energy change, comparing to wild type of RC, we can reproduce the observed quantum yields in the DH mutants. With a triple mutant of *Rb.capsulatus*,<sup>24</sup> S(L178)K/G(M201)D/L(M212)H (denoted KDH), 62% of ET was observed to the *L*-side bacteriopheophytin, 23% to the *M*-side, and 15% was returning to the ground state. It is expected that in this mutation, it is the S(L178)K mutation which lowers the free energy of the  $P^+B_M^-$  state. To characterize this change of energy level we have used the value  $\epsilon_2 = 700 \text{ cm}^{-1}$ . This is the only change in parameters comparing to the previous mutant to elucidate the quantum yields.

For the F(L181)Y/Y(M208)F/L(M212)H (denoted YFH) mutant of *Rb.capsulatus*,<sup>23</sup> 60% of ET was observed to the *L*-side bacteriopheophytin, 30% to the *M*-side and 10% was returning to the ground state. There is an assumption that this mutation has the similar effect as the previously described one. To characterize this mutation we increase the energy  $\epsilon_3$  from the value  $\epsilon_3 = -450 \text{ cm}^{-1}$  to the value  $\epsilon_3 = 400 \text{ cm}^{-1}$ . It is also necessary to lower the free energy of  $P^+B_M^-$  state to the value  $\epsilon_2 = 550 \text{ cm}^{-1}$ . With these changes our model is able to reproduce the observed quantum yields.

For the G(M201)D (denoted D) single mutant of *Rb.capsulatus*, which raises the free energy of  $P^+B_L^-$ ,<sup>25-27</sup> there is no experimental evidence of ET to the *M*-side. Because of difficulties with detection of small ET to *M*-side in mutants

that retain a native  $H_L$ , there is, however, a probability of 5%–10% of ET to this side.<sup>28</sup> Our analysis gives similar quantum yields for the  $D$  mutant as for the  $DH$  mutant, which is not in accordance with the experimental results.

### B. Parallel superexchange/sequential model

Up to now we have assumed that ET has sequential character in both branches of reaction centers. Now we would like to analyze the contribution from a superexchange mechanism to both  $M$  and  $L$  side ET. This option can be introduced by the additional sink parameters at site 1.

The formula for superexchange rate based on different approximations was derived in the earlier works.<sup>13,29–35</sup> Using the formula derived in the work,<sup>29</sup> which is proper for the bath used in the presented model, we get the rate constant which characterizes the superexchange mechanism at the  $L$  branch in the following form:

$$k_{st} = \frac{2\pi}{\hbar} \frac{V_{13}^2 V_{35}^2}{E^2} \left( \frac{1}{4\pi\lambda_{15}k_B T} \right)^{1/2} \exp(-S_{15}) \times \sum_{n=0}^{\infty} \frac{S_{15}^n}{n!} \exp\left[ -\frac{(G_{51} + \lambda_{15} + n\hbar\omega_{15})^2}{4\lambda_{15}k_B T} \right], \quad (25)$$

where

$$E = \epsilon_1 - \epsilon_3 - \tilde{\lambda}_{13} - A(\epsilon_1 - \epsilon_5 - \tilde{\lambda}_{15}), \quad (26)$$

$$\tilde{\lambda}_{13} = S_{13}\hbar\omega_{13} + \lambda_{13}, \quad (27)$$

$$\tilde{\lambda}_{15} = S_{15}\hbar\omega_{15} + \lambda_{15}, \quad (28)$$

$$A = \frac{\sqrt{S_{13}S_{15}}\hbar^2\omega_{15}^2 + 2\sqrt{\lambda_{13}\lambda_{15}}k_B T}{S_{15}\hbar^2\omega_{15}^2 + 2k_B T\lambda_{15}}. \quad (29)$$

Similar to the work,<sup>17</sup> for the numerical computations the value,  $S_{15} = S_{14} = 1$ ,  $\hbar\omega_{15} = \hbar\omega_{14} = 1500 \text{ cm}^{-1}$ , and  $\lambda_{15} = \lambda_{14} = 1600 \text{ cm}^{-1}$  were taken. All other parameters were as defined in the Sequential Model. With these parameters we get  $A = \sqrt{0.5}$ . Changing  $3 \rightarrow 2$  and  $5 \rightarrow 4$  in Eqs. (25)–(29) we get the expression for  $k_{SM}$  which characterizes the superexchange mechanism in the  $M$  branch of the RC. In the case when we assume that in the  $M$  branch the ET have superexchange character and in the  $L$  branch the ET have sequential character, the parameters  $R$  and  $K$  have the form,

$$K = \frac{k_{13}k_{35}}{k_{SM}(k_{31} + k_{35})}, \quad R = \frac{\hbar k_{13}k_{35}}{2\Gamma_1(k_{31} + k_{35})}. \quad (30)$$

The results of numerical calculations of QY for a parallel sequential and a superexchange mechanism in both branches of RC for different samples of RC are collected in Table II.

### C. Asymmetry in electronic couplings

There is also the possibility that the asymmetry of the electronic factors can contribute to the unidirectionality.<sup>11,36–39</sup> When we assume, similarly as in the work,<sup>36</sup> that there is an asymmetry in the electronic couplings  $V_{13}/V_{12} \approx 2.8$  and  $V_{35}/V_{24} \approx 2.1$  and also using the parameters:

TABLE II. Computed constants  $1/k_{SL}$ ,  $1/k_{SM}$ , and quantum yields for wild type and mutants RC's.<sup>a</sup>

Sample	T (K)	$1/k_{SL}$ (ps)	$1/k_{SM}$ (ps)	$\phi_L$	$\phi_M$	$\phi_G$
WT	295	75	764	0.968	0.019	0.013
WT	200	70	729	0.983	0.005	0.012
D	295	1147	764	0.674	0.189	0.137
D	200	1069	729	0.576	0.126	0.298
DH	295	303	764	0.709	0.168	0.123
DH	200	290	729	0.623	0.11	0.267
KDH	295	303	597	0.646	0.242	0.112
KDH	200	290	570	0.583	0.169	0.248
YFH	295	220	386	0.607	0.318	0.075
YFH	200	210	368	0.597	0.245	0.158

<sup>a</sup>Parallel sequential and superexchange mechanism in both branches was assumed. Constants  $1/k_{ij}$  and site energy parameters are given in Table I.

$\hbar\omega_{ij} = 1500 \text{ cm}^{-1}$ ,  $V_{12} = 11.4 \text{ cm}^{-1}$ ,  $V_{13} = 32 \text{ cm}^{-1}$ ,  $V_{24} = 28 \text{ cm}^{-1}$ ,  $V_{35} = 59 \text{ cm}^{-1}$ ,  $S_{ij} = 0.5$ ,  $S_{15} = S_{14} = 1$ ,  $\epsilon_1 = 0$ ,  $\epsilon_2 = 800 \text{ cm}^{-1}$ ,  $\epsilon_3 = -450 \text{ cm}^{-1}$ ,  $\epsilon_5 = -2000 \text{ cm}^{-1}$ ,  $\epsilon_4 = -1000 \text{ cm}^{-1}$ ,  $\lambda_{ij} = 800 \text{ cm}^{-1}$ ,  $\lambda_{15} = \lambda_{14} = 1600 \text{ cm}^{-1}$ , and  $2\Gamma_1/\hbar = (170 \text{ ps})^{-1}$ , we get the corresponding quantum yields and constants  $k_{ij}$  for the wild type of RC at  $T = 295 \text{ K}$ :  $\Phi_O \approx 0.014$ ,  $\Phi_M \approx 0.002$ ,  $\Phi_L \approx 0.984$ ,  $k_{13} = (2.34 \text{ ps})^{-1}$ ,  $k_{35} = (0.9 \text{ ps})^{-1}$ ,  $k_{12} = (762 \text{ ps})^{-1}$ ,  $k_{24} = (4.5 \text{ ps})^{-1}$ ,  $k_{SL} = (76 \text{ ps})^{-1}$ ,  $k_{SM} = (27 \text{ ns})^{-1}$ . At a temperature  $T = 200 \text{ K}$  we have:  $\Phi_G \approx 0.0122$ ,  $\Phi_M \approx 0.0004$ ,  $\Phi_L \approx 0.9874$ ,  $k_{13} = (2.1 \text{ ps})^{-1}$ ,  $k_{35} = (1.1 \text{ ps})^{-1}$ ,  $k_{12} = (4 \text{ ns})^{-1}$ ,  $k_{24} = (5.4 \text{ ps})^{-1}$ ,  $k_{SL} = (70 \text{ ps})^{-1}$ ,  $k_{SM} = (25 \text{ ns})^{-1}$ .

However, if there is only one asymmetry in the electronic couplings we have the following QY and  $k_{ij}$  for wild type of RC at  $T = 295 \text{ K}$ :  $\Phi_G \approx 0.012$ ,  $\Phi_M \approx 0.111$ ,  $\Phi_L \approx 0.877$ ,  $k_{13} = (2.34 \text{ ps})^{-1}$ ,  $k_{35} = (0.9 \text{ ps})^{-1}$ ,  $k_{12} = (18 \text{ ps})^{-1}$ ,  $k_{24} = (4 \text{ ps})^{-1}$ ,  $k_{SL} = (76 \text{ ps})^{-1}$ ,  $k_{SM} = (2.7 \text{ ns})^{-1}$ . At room temperature  $T = 200 \text{ K}$  we have  $\Phi_G \approx 0.011$ ,  $\Phi_M \approx 0.110$ ,  $\Phi_L \approx 0.879$ ,  $k_{13} = (2.1 \text{ ps})^{-1}$ ,  $k_{35} = (1.1 \text{ ps})^{-1}$ ,  $k_{12} = (17 \text{ ps})^{-1}$ ,  $k_{24} = (5 \text{ ps})^{-1}$ ,  $k_{SL} = (70 \text{ ps})^{-1}$ ,  $k_{SM} = (2.4 \text{ ns})^{-1}$ . In the computations the following parameters were utilized:  $\hbar\omega_{ij} = 1500 \text{ cm}^{-1}$ ,  $V_{12} = 11.4 \text{ cm}^{-1}$ ,  $V_{13} = 32 \text{ cm}^{-1}$ ,  $V_{24} = 28 \text{ cm}^{-1}$ ,  $V_{35} = 59 \text{ cm}^{-1}$ ,  $S_{ij} = 0.5$ ,  $S_{15} = S_{14} = 1$ ,  $\epsilon_1 = 0$ ,  $\epsilon_2 = -450 \text{ cm}^{-1}$ ,  $\epsilon_3 = -450 \text{ cm}^{-1}$ ,  $\epsilon_5 = -2000 \text{ cm}^{-1}$ ,  $\epsilon_4 = -2000 \text{ cm}^{-1}$ ,  $\lambda_{ij} = 800 \text{ cm}^{-1}$ ,  $\lambda_{15} = \lambda_{14} = 1600 \text{ cm}^{-1}$ , and  $2\Gamma_1/\hbar = (170 \text{ ps})^{-1}$ .

## VI. DISCUSSION

The interesting to note is a contradiction between the observed and computed QY in  $D$  and  $DH$  mutant from point of view the theory presented in the paper. Up to now it was assumed that the only difference between these two mutants is in the site energy  $\epsilon_5$ . In the sequential model this difference is demonstrated in constant  $k_{35}$  where a free energy difference  $G_{35}$  has value  $2480 \text{ cm}^{-1}$  in the  $D$  mutant and  $1480 \text{ cm}^{-1}$  in the  $DH$  mutant. Because of the high frequency mode is present in the bath this amount of energy can be relatively easily absorbed by the bath. So in both cases we observe a rapid ET from site 3 to site 5. However, quantum yields  $\Phi_L$  and  $\Phi_M$  are more sensitive to the first step of ET

and so small changes in the second step of ET have no strong influence on the QY. The result is that our model predicts the similar QY's in these two mutants.

However, there is a possibility to elucidate the observed QY in the *D* mutant which can be in accordance with observed  $P^*$  lifetime temperature dependence. Experimental data indicate a small temperature dependence of the lifetime of  $P^*$  state in a temperature range 77–295 K. The lifetime of  $P^*$  state is about 7.6 ps at 285 K and 10 ps at 77 K in the *D* mutant.<sup>40</sup> From these data a value of  $\epsilon_3$  can be estimated to be about 200–500  $\text{cm}^{-1}$  above  $P^*$  and this case was already analyzed in the foregoing sections.

The other possibility what we have to investigate now is that  $\epsilon_3$  can be 200–500  $\text{cm}^{-1}$  below  $P^*$ . In this case the increase of lifetime of the *D* mutant, in comparison with the wild type, ought to be caused also by changes in the electronic couplings. This possibility leads to, assuming the changes in comparison with wild type in parameters,  $\epsilon_3 = -200 \text{ cm}^{-1}$  and  $V_{13} = 16 \text{ cm}^{-1}$  to the quantum yields and constants  $k_{ij}$  at  $T = 295 \text{ K}$ :  $\Phi_G \approx 0.068$ ,  $\Phi_M \approx 0.093$ ,  $\Phi_L \approx 0.839$ ,  $k_{13} = (13.5 \text{ ps})^{-1}$ ,  $k_{35} = (1 \text{ ps})^{-1}$ ,  $k_{12} = (96.7 \text{ ps})^{-1}$ ,  $k_{24} = (1 \text{ ps})^{-1}$ ,  $k_{SL} = (958 \text{ ps})^{-1}$ ,  $k_{SM} = (0.7 \text{ ns})^{-1}$ . At temperature  $T = 200 \text{ K}$  we have  $\Phi_G \approx 0.076$ ,  $\Phi_M \approx 0.033$ ,  $\Phi_L \approx 0.891$ ,  $k_{13} = (14.5 \text{ ps})^{-1}$ ,  $k_{35} = (1.2 \text{ ps})^{-1}$ ,  $k_{12} = (0.5 \text{ ns})^{-1}$ ,  $k_{24} = (1.2 \text{ ps})^{-1}$ ,  $k_{SL} = (0.9 \text{ ns})^{-1}$ ,  $k_{SM} = (0.7 \text{ ns})^{-1}$ .

Because similar temperature dependence of  $P^*$  lifetime is observed also for the DH mutant<sup>40</sup> the similar arguments ought to be applied for this mutant. Yet for this analysis we have to use the model with more sites of electron localization than there are in our model. It is because in the DH mutant the free energy levels  $\epsilon_3$  and  $\epsilon_5$  can be nearby and so the backward reaction from site 5 cannot be neglected.

The observed QY can be reproduced of course also by the selection of another parameter. However, currently there is practically nothing known about the change of electronic coupling in the mutants to proceed in the discussion about these parameters.

In case that there is a strong asymmetry in the electronic couplings for the wild type of RC, the QY of the mutants must be elucidated with the other energetic parameters than the ones used in the present work. We believe that to discriminate between these options the determination of the temperature dependence of QY can be most valuable.

The assignment of free energies arrangement can be verified by similar temperature measurements. For this purpose the temperature effects on ET were computed. We have predicted the quantum yield for *Rb.capsulatus* mutant at 200 K. Moreover, the computed temperature dependence of ET with the selected energy arrangement shows that the asymmetry of primary charge transfer is increasing with decreasing the temperature in the case of the wild type of RC. We have demonstrated also a strong increase of the ground state recombination with a decrease of temperature in the case of double and triple mutants of *Rb.capsulatus* in the case where free energy  $\epsilon_3$  is above  $P^*$ . At low temperature we have found the electron localized at site 1 with greater probability and so there is a greater chance that the system decays to the ground state. The reason is that the ratio of backward to

forward reaction is greater at low temperature than at high temperature.

In a case when the free energy  $\epsilon_3$  is below  $P^*$  the increase of *L*-branch ET is predicted. It is because in the *L* branch the ratio of backward to forward reactions have opposite character as in the previous case. The results were found to be dependent on changes of parameter  $\Gamma_1$ , assumed to be small, in the considered temperature range.

At this point we would like to discuss the possibility of partially coherent ET. In this case we assume that the reorganization energies  $E_{12}^\alpha$  in the Eq. (14) are zero. In this case parameters  $K$  and  $R$  have the forms,

$$K = \frac{k_{13}k_{35} \left[ V_{12}^2 \left( k_{24} + \frac{2\Gamma_1}{\hbar} \right) + k_{24}(\Gamma_1^2 + G_{12}^2) \right]}{V_{12}^2 k_{24} (k_{31} + k_{35}) (k_{24} + 2\Gamma_1/\hbar)}$$

$$R = \frac{\hbar k_{13}k_{35}}{2\Gamma_1 (k_{31} + k_{35})} \quad (31)$$

If the free energy difference  $G_{12}$  is large enough we will get the similar expressions for  $R$  and  $K$  parameters as in a case when the superexchange mechanism in the *M* branch is assumed,

$$K = \frac{k_{13}k_{35}}{k_{\text{COH}}(k_{31} + k_{35})}, \quad R = \frac{\hbar k_{13}k_{35}}{2\Gamma_1 (k_{31} + k_{35})}, \quad (32)$$

where

$$k_{\text{COH}} = \frac{2\pi}{\hbar} \frac{V_{12}^2 V_{24}^2}{G_{12}^2} \left( \frac{1}{4\pi\lambda_{24}k_B T} \right)^{1/2} \exp(-S_{24}) \sum_{n=0}^{\infty} \frac{S_{24}^n}{n!}$$

$$\times \exp \left[ \frac{(G_{42} + \lambda_{24} + n\hbar\omega_{24})^2}{4\lambda_{24}k_B T} \right]. \quad (33)$$

Assuming that also reorganization energies  $E_{13}^\alpha$  are zero we get the coherent sequential electron transfer in both branches. This case was already described in our previous work.<sup>6</sup> In the present study the coherent ET was derived from Eq. (13) as a special case. At these specific conditions the initial state is a superposition of eigenstates of the total Hamiltonian  $H$  and the population probabilities  $P_i(t)$  oscillate with frequencies that are functions of  $V_{ij}^2$  and  $G_{ij}^2$  parameters. Moreover, the states above  $P^*$  can be reached without thermal populations. Opposite to this case is an incoherent sequential ET where the memory kernels  $W_{ij}(t)$  in Eq. (13) are damped sufficiently fast, and Eq. (13) can be changed to the ordinary rate equation. At these circumstances if the  $P^+B^-$  state is above  $P^*$ , then it can be reached only via thermal population in the absence of the superexchange mechanism.

## VII. CONCLUSIONS

The asymmetry of electron transfer in photosynthetic reaction centers can be explained in several ways. One approach<sup>5,6</sup> assumes that the stochastic fluctuation does not depend on the localization of the electron in the branch. In other words the transfer of electrons has a hot character.<sup>41</sup>

The second possible explanation, presented in this paper, is based on the model where we suggest that in the RC the vibrational modes with a fast enough relaxation are present and the system can partially relax to a thermal equilibrium after each ET step. We think that both the previous models<sup>5,6</sup> and the presented model give the qualitatively same ET asymmetry dependence on the free energy and electronic coupling parameters. This means that using slightly different parameters which characterized the models we can get the same quantum yields at high temperature and also similar  $k_{ij}$ . The difference in the parameters and also the interplay between the forward and backward kinetics, which depends on the temperature in incoherent sequential model and does not depend on temperature in the hot electron transfer case, predicts a different dependence of ET asymmetry on temperature in the incoherent sequential in comparison to the model where electron transfer has hot or coherent character.

However, as it was mentioned earlier the presented model excludes on the studied time scale the repopulation processes of electron accepting sites. This exclusion requires the introduction of imaginary part of energy levels both to explain the observed asymmetry and to have physically meaningful occupational probabilities. Without the imaginary part the solution of equations for the occupational probability can lead to the negative values.

Using this model we have derived the generalized master equations (GME), which describe the primary charge transfer in the photosynthetic reaction centers. Usually these integrodifferential equations (GME) are changed to differential equations (master equations) without a verification of correctness of this step. To justify this change it has to be shown that the memory kernels  $W_{ij}(t)$  fulfilled certain conditions. Specifically, that memory kernel is damped very quickly in comparison to the relaxation of system to a steady state.<sup>42</sup> However, a verification of this condition is questionable if for the description of surrounding medium are used only two vibrational modes, which is the most common case.

From our analysis follows that the superexchange mechanism operating in parallel with sequential process must be used to get a reliable QY at low temperature. There is also possibility that with decreasing temperature the reorganization energy is also decreasing and so at low temperature the incoherent sequential ET is changed to coherent sequential and it can have the similar contribution to QY as the superexchange mechanism.

The observed QY in DH, KDH, and YFH mutants can be elucidated by changing the free energy of  $P^+B_L^-$  or  $P^+B_M^-$  state relative to the wild type. However, this explanation is not attainable because of inconsistency between the observed and the theoretically predicted QY in the *D* mutant. As it was shown in our analysis only the changes in energy cannot explain the differences in the observed QY in the *D* and DH mutants. There is a strong possibility that changes in the quantum yields in the *D*, DH, and KDH mutants are caused not only by changes of the free energy differences but the important role can play also the changes in the electronic couplings.

To give the more credible information about the free

energy arrangement and possible asymmetry in the electronic coupling terms we have to compare theoretical prediction with observed quantum yields also in the low temperature regime.

## ACKNOWLEDGMENTS

The authors thanks Dr. M. Fabian and Dr. D. Holten for useful comments. This work has been supported by the Slovak Scientific Grant Agency, Grant No. 7043.

- <sup>1</sup>L. N. M. Duysens, *Biochim. Biophys. Acta* **19**, 188 (1956).
- <sup>2</sup>H. Michel, K. A. Weyer, H. Gruenberg, and F. Lottspeich, *EMBO J.* **4**, 1667 (1985).
- <sup>3</sup>K. A. Weyer, F. Lottspeich, H. Gruenberg, F. S. Lang, D. Oesterhelt, and H. Michel, *EMBO J.* **6**, 2197 (1987).
- <sup>4</sup>J. Deisenhofer and H. Michel, *EMBO J.* **8**, 2149 (1989).
- <sup>5</sup>R. Pinčák and M. Pudlak, *Phys. Rev. E* **64**, 031906 (2001).
- <sup>6</sup>M. Pudlak and R. Pinčák, *Chem. Phys. Lett.* **342**, 587 (2001).
- <sup>7</sup>M. Sparpaglione and S. Mukamel, *J. Chem. Phys.* **88**, 3263 (1988).
- <sup>8</sup>R. Zwanzig, *Physica (Amsterdam)* **30**, 1109 (1964).
- <sup>9</sup>N. Hashitsume, P. Shibata, and M. Shingu, *J. Stat. Phys.* **17**, 253 (1972).
- <sup>10</sup>V. Čapek and V. Szöcs, *Phys. Status Solidi B* **125**, K137 (1984).
- <sup>11</sup>M. E. Michel-Beyerle, M. Plato, J. Deisenhofer, H. Michel, M. Bixon, and J. Jortner, *Biochim. Biophys. Acta* **932**, 52 (1988).
- <sup>12</sup>J. Jortner, *J. Chem. Phys.* **64**, 4860 (1976).
- <sup>13</sup>Y. Hu and S. Mukamel, *J. Chem. Phys.* **91**, 6973 (1989).
- <sup>14</sup>V. Čapek and V. Szöcs, *Czech. J. Phys., Sect. B* **36**, 1182 (1986).
- <sup>15</sup>M. Marchi, J. N. Gehlen, D. Chandler, and M. D. Newton, *J. Am. Chem. Soc.* **115**, 4178 (1993).
- <sup>16</sup>S. Tanaka and R. A. Marcus, *J. Phys. Chem. B* **101**, 5031 (1997).
- <sup>17</sup>M. Bixon, J. Jortner, and M. E. Michel-Beyerle, *Chem. Phys.* **197**, 389 (1995).
- <sup>18</sup>R. G. Alden, W. W. Parson, Z. T. Chu, and A. Warshel, *J. Phys. Chem.* **100**, 16761 (1996).
- <sup>19</sup>M. R. Gunner, A. Nicholls, and B. Honig, *J. Phys. Chem.* **100**, 4277 (1996).
- <sup>20</sup>M. A. Thompson, M. C. Zerner, and J. Fajer, *J. Am. Chem. Soc.* **113**, 8210 (1991).
- <sup>21</sup>M. Marchi, J. N. Gehlen, D. Chandler, and M. Newton, *Science* **263**, 499 (1994).
- <sup>22</sup>M. R. A. Blomberg, P. E. M. Siegbahn, and G. T. Babcock, *J. Am. Chem. Soc.* **120**, 8812 (1998).
- <sup>23</sup>Ch. Kirmaier, Ch. He, and D. Holten, *Biochemistry* **40**, 12132 (2001).
- <sup>24</sup>Ch. Kirmaier, D. Weems, and D. Holten, *Biochemistry* **38**, 11516 (1999).
- <sup>25</sup>W. W. Parson, Z. T. Chu, and A. Warshel, *Biochim. Biophys. Acta* **1017**, 251 (1990).
- <sup>26</sup>C. Kirmaier, A. Cua, Ch. He, D. Holten, and D. F. Bocian, *J. Phys. Chem. B* **106**, 495 (2002).
- <sup>27</sup>C. Kirmaier, P. D. Laible, K. Czarniecki, A. N. Hata, D. K. Hanson, D. F. Bocian, and D. Holten, *J. Phys. Chem. B* **106**, 1799 (2002).
- <sup>28</sup>D. Holten (private communication).
- <sup>29</sup>J. S. Joseph and W. Bialek, *J. Phys. Chem.* **97**, 3245 (1993).
- <sup>30</sup>R. Islampour and S. H. Lin, *J. Phys. Chem.* **95**, 10261 (1991).
- <sup>31</sup>M. Bixon and J. Jortner, *J. Chem. Phys.* **107**, 5154 (1997).
- <sup>32</sup>L. D. Zusman and D. N. Beratan, *J. Chem. Phys.* **110**, 10468 (1999).
- <sup>33</sup>H. Sumi, *J. Electroanal. Chem.* **438**, 11 (1997).
- <sup>34</sup>A. Kimura and T. Kakitani, *Chem. Phys. Lett.* **298**, 241 (1998).
- <sup>35</sup>R. Egger, C. H. Mak, and U. Weiss, *Phys. Rev. E* **50**, R655 (1994).
- <sup>36</sup>M. Plato, K. Möbius, M. E. Michel-Beyerle, M. Bixon, and J. Jortner, *J. Am. Chem. Soc.* **110**, 7279 (1988).
- <sup>37</sup>J. Hasegawa and H. Nakatsuji, *J. Phys. Chem. B* **102**, 10420 (1998).
- <sup>38</sup>N. Ivashin, B. Källebring, S. Larsson, and Ö. Hansson, *J. Phys. Chem. B* **102**, 5017 (1998).
- <sup>39</sup>D. Kolbasov and A. Scherz, *J. Phys. Chem. B* **104**, 1802 (2000).
- <sup>40</sup>K. Czarniecki, C. Kirmaier, D. Holten, and D. F. Bocian, *J. Phys. Chem. A* **103**, 2235 (1999).
- <sup>41</sup>H. Sumi, *Phys. Rev. Lett.* **50**, 1709 (1983).
- <sup>42</sup>R. Kubo, M. Toda, and N. Hashitsume, *Statistical Physics II, Nonequilibrium Statistical Mechanics* (Springer-Verlag, Heidelberg, 1998).